April 25, 2021 KB

Fixation and effective size in a haploid-diploid population with asexual reproduction

***Kazuhiro Bessho, **Sarah P. Otto**

* *Saitama Medical University, 38 Morohongo Moroyama-machi, Iruma-gun, Saitama 350-0495, Japan*

***Department of Zoology, The University of British Columbia, Vancouver, BC, V6T 1Z4, Canada*

* besshokazuhiro.reserch@gmail.com; (+81) 049-276-2030

** otto@zoology.ubc.ca; (+1) 604-822-2778

*Corresponding author

besshokazuhiro.reserch@gmail.com (KB)

*Co-corresponding author

otto@zoology.ubc.ca (SPO)

***Keywords*:** haploid-diploid life cycle, Wright-Fisher model, fixation probability, variance effective population size, class reproductive value

Abstract

The majority of population genetic theory assumes fully haploid or diploid organisms with obligate sexuality, despite complex life cycles with alternating generations being commonly observed. To reveal how natural selection and genetic drift shape the evolution of haploid-diploid populations, we analyze a stochastic genetic model for populations that consist of a mixture of haploid and diploid individuals, allowing for asexual reproduction and niche separation between haploid and diploid stages. Applying a diffusion approximation, we derive the fixation probability and describe its dependence on the reproductive values of haploid and diploid stages, which depend strongly on the extent of asexual reproduction in each phase and on the ecological differences between them.

1. Introduction

Sexual reproduction in eukaryotes generally consists of an alternation of generations, where meiosis halves the number of chromosomes to produce haploids and syngamy brings together haploid gametes to produce diploids. The extent of development in each ploidy phase varies substantially (Bell 1982; 1994). In diplontic organisms, at one extreme, development and growth occur only in the diploid phase, as is observed in most animals. Haplontic organisms, at the other extreme, undergo mitotic growth only in the haploid stage, as is seen in some green algae. In between these extremes, many terrestrial plants, macroalgae, and fungi exhibit both haploid and diploid growth (haploid-diploid life cycles). These stages are typically free living in macroalgae, with either macroscopically similar (isomorphic) or distinct (heteromorphic) forms in the haploid and diploid stage (Raper and Flexer 1970; Wilson 1981; Mable and Otto 1998; Coelho 2007).

To explain variation in life cycles, several theoretical models have analyzed the deterministic dynamics of a modifier allele that alters the time spent in haploid and diploid phases (e.g., Perrot et al. 1991; Otto and Goldstein 1992; Goldstein 1992; Otto 1994; Orr and Otto 1994; Jenkins and Kirkpatrick 1995; Otto and Marks 1996; Scott and Rescan 2017). However, there are some gaps between these models and the complexities seen in many haploid-diploid species. For example, these models often treat haploid and diploid individuals as ecologically equivalent, despite the frequent observation of niche differences and seasonal shifts in prevalence (e.g., Slocum 1980; Dethier 1981). Most of these models also assume obligate sexuality (but see Otto and Marks 1996), despite asexuality being frequently observed among haploid-diploid species (“asexual looping”). Furthermore, while several models have explored how haploid-diploid life cycles might evolve, the impact of haploid-diploid life cycles on

evolutionary processes remains underexplored (see, e.g., Bessho and Otto 2017 on the impact on fixation probabilities and Immler et al. 2012 on the maintenance of variation).

Here we contribute to evolutionary theory for haploid-diploid populations by calculating the fixation probability of mutations using a stochastic genetic model. This builds upon our previous work (Bessho and Otto 2017) by accounting for asexual looping and niche differences between ploidy phases, both of which are common in macroalgae (Bell 1982; de Wreede and Klinger 1988; Hawkes 1990). Haploid and diploid phases often differ physiologically, and even isomorphic haploids and diploids may differ ecologically (Hannach and Santelices 1985; Destombe et al. 1993; Dyck and de Wreede 2006; Thornber et al., 2006; Vieira et al. 2018). We therefore explore different forms of density dependence, acting either globally on the total population size (as in Bessho and Otto 2017) or locally on the population size of haploids and diploids separately (Figure 1). We show that the fate of a mutation depends strongly on the reproductive values of haploids and diploids, which in turn depend on the extent of asexual reproduction and ecological differences between the phases.

2. Model

In Bessho and Otto (2017), we calculated the fixation probabilities by tracking the dynamics of a resident allele (R) and a mutant allele (M) in haploid and diploid individuals, using both a Wright-Fisher and a Moran model. In that model, reproduction was obligately sexual, individuals were ecologically equivalent, and the total population size was held constant (global density dependence). Below, we calculate the fixation probability by first considering asexual reproduction in each phase, assuming that haploids and diploids are ecologically equivalent (global population regulation), and then determine how these results are affected by niche differences (local population regulation that is ploidy specific).

83

84 2.1. Haploid-diploid Wright-Fisher model with global regulation and asexual looping

85 Let $X_{(GT)}(t)$ be a random variable that represents the number of individuals with
86 "genotype" (*GT*) at time *t* with resident (*R*) and mutant alleles (*M*), and let $x_{(GT)}(t)$ represent a
87 particular outcome of this random variable. In the global regulation model, we assume a constant
88 population, $x_R + x_M + x_{RR} + x_{RM} + x_{MM} = N_{tot}$, that is strictly regulated regardless of the
89 ploidy of the individuals.

90 The reproductive output and the degree of asexuality are characterized by $w_{(GT)}$ and
91 a_H for haploids [(*GT*) = *R* or *M*] and $w_{(GT)}$ and a_D for diploids [(*GT*) = *RR*, *RM*, and *MM*].
92 Specifically, diploid individuals produce $(1 - a_D)w_{(GT)}$ haploid spores (sexual reproduction)
93 and $a_D w_{(GT)}$ diploid offspring (asexual loop). Similarly, haploids produce $(1 - a_H)w_{(GT)}/2$
94 female gametes (sexual reproduction) and $a_H w_{(GT)}$ haploid offspring (asexual loop), where we
95 assume that the species is monoecious and invests equal resources in male and female gametes.
96 During syngamy, we assume that male gametes are not limiting, that mating is random, and that
97 female gametes are successfully fertilized with male gametes, at a rate $f_{(GT)}$ [(*GT*) = *R* or *M*],
98 becoming diploid zygotes. For clarity, we describe the model with non-overlapping generations,
99 although we note that overlapping generations can be considered by including surviving adults in
100 the counts of asexual offspring ($a_D w_{(GT)}$ and $a_H w_{(GT)}$).

101 We define the selection coefficient ($s_{(GT)}$) and the degree of dominance (h) acting upon
102 the mutant allele such that: $f_M = f_R\left(1 - s_M^f\right)$, $w_M = w_R(1 - s_M^w)$, $w_{RM} = w_{RR}(1 - s_{RM}^w)$,
103 $w_{MM} = w_{RR}(1 - s_{MM}^w)$, and $h = s_{RM}^w / s_{MM}^w$. To perform the diffusion approximation, we assume
104 that selection is weak, $s_M^f = \epsilon \tilde{s}_M^f$ and $s_{(GT)}^w = \epsilon \tilde{s}_{(GT)}^w$, where ϵ is a small parameter.

105

106 2.2. Haploid-diploid Wright-Fisher model with local regulation and asexual looping

We then consider the case where density dependence regulates haploid and diploid populations separately, which may occur if they have different resource needs or utilize different habitats or microhabitats (for short-hand, we refer to this case as "local regulation"). More specifically, we assume that the population size of haploids and diploids is separately regulated and remains constant N_H and N_D ($x_R + x_M = N_H$ and $x_{RR} + x_{RM} + x_{MM} = N_D$), respectively. We set $N_H + N_D = N_{tot}$, $\hat{\rho}_H^L = N_H/N_{tot}$, and $\hat{\rho}_D^L = N_D/N_{tot}$, which will then allow us to compare the results of local and global regulation. Holding population sizes constant is assumed strictly for mathematical convenience but may be reasonable for populations whose sizes are strongly regulated by the availability of appropriate habitat.

3. Fixation probability in a haploid-diploid population

3.1. Fixation probability in the global regulation model

The fixation probability in a haploid-diploid population can be derived using a diffusion approximation (Bessho and Otto 2017), but doing so requires that we approximate the dynamics to reduce the dimensionality from four variables ($x_R, x_M, x_{RR}, x_{RM}, x_{MM}$, which sum to N_{tot}) down to one. We do so by using a separation of time scales, deriving the first and second moments of the mutant allele frequency. Specifically, we transform the number of individuals of each genotype, $x_{(GT)}$, into new variables that allow us to separate the slower evolutionary dynamics and the faster ecological dynamics (Appendix A):

$$p_{ave} = c_H\, p_H + c_D\, p_D, \tag{1a}$$

$$\delta_p = p_D - p_H, \tag{1b}$$

$$\eta_{HW} = 1 - \frac{1}{2p_D(1-p_D)} \frac{x_{RM}}{x_{RR} + x_{RM} + x_{MM}}, \tag{1c}$$

$$\rho_H = \frac{x_R + x_M}{N_{tot}}, \tag{1d}$$

where p_{ave} indicates the average allele frequency of haploids and diploids weighted by the class reproductive values (c_H and c_D, where $c_H + c_D = 1$, see next paragraph), δ_p indicates the difference in allele frequencies between haploids and diploids, η_{HW} indicates the departure from the Hardy-Weinberg equilibrium in diploids, and ρ_H indicates the frequency of haploids in the population. Within these equations, the frequencies of mutant alleles in haploids and diploids are $p_H = x_M/(x_R + x_M)$ and $p_D = \left(\frac{x_{RM}}{2} + x_{MM}\right)/(x_{RR} + x_{RM} + x_{MM})$. As similar variables are used in the model with local population regulation, we use superscripts to indicate the form of population regulation ("*Model*" is *G* for global or *L* for local regulation).

The class reproductive values of haploids and diploids are defined as follows. In linear models, "reproductive value" is a measure of the expected fraction of the population in the long-term future that descends from an individual of a particular type (e.g., age or stage class). Class reproductive values, as defined by Taylor (1990) and Rousset (2004, p.153), scale these individual reproductive values up to the whole population of each class (i.e., the product of the individual reproductive values times the class size). In the models considered here, the dynamics are non-linear because of competition for resources (N_{tot}). Nevertheless, we can approximate reproductive values by assuming that the population is near equilibrium with only resident alleles and by holding the strength of competition constant (see Supplementary *Mathematica* file for all calculations). Doing so, we find that the class reproductive values of haploids and diploids, expressed as proportions that sum to one, are:

$$c_H^G = \frac{(1 - a_H)\frac{f_R}{2} w_R (\hat{\rho}_H^G)^2}{(1 - a_H)\frac{f_R}{2} w_R (\hat{\rho}_H^G)^2 + (1 - a_D) w_{RR} (\hat{\rho}_D^G)^2}, \tag{2a}$$

$$c_D^G = \frac{(1-a_D)w_{RR}(\hat{\rho}_D^G)^2}{(1-a_H)\frac{f_R}{2}w_R(\hat{\rho}_H^G)^2 + (1-a_D)w_{RR}(\hat{\rho}_D^G)^2}. \quad (2b)$$

where $\hat{\rho}_H^G = 1 - \hat{\rho}_D^G$ is the equilibrium frequency of haploids in the global model (Eq. A.4). As a special case of interest, when populations are purely sexual ($a_H = a_D = 0$), we can plug the equilibrium for $\hat{\rho}_H^G$ from Eq. (A.4) into (2) and show that $c_H^G = c_D^G = 1/2$.

As discussed in Appendix A (see also Bessho and Otto 2017), equations (2) provide the only weights that allow ecological and evolutionary time scales to be separated when calculating the average allele frequency in equation (1a), which is why we take that to be the evolutionarily relevant average. Although one might initially think that diploids should count twice as much because they contain two allele copies and that the evolutionarily relevant average allele frequency would depend on the population sizes of haploids and diploids, a strict alternation of generations ($a_H = a_D = 0$) ensures that haploids and diploids contribute equally to long-term future generations, so that their reproductive values are equal and the evolutionarily relevant average allele frequency is $p_{ave} = (1/2)p_H + (1/2)p_D$ (Bessho and Otto 2017).

As with our previous model, we can track the slow evolutionary dynamics for the expected change in average allele frequency p_{ave} under weak selection, once the fast ecological dynamics have stabilized, as which point we can show that there are similar allele frequencies in haploids and diploids ($\delta_p \approx 0$), diploids are approximately at Hardy-Weinberg equilibrium ($\eta_{HW} \approx 0$), and the ratio of haploids is similar among mutant and resident genotypes ($\rho_H \approx \hat{\rho}_H^G$) (Appendix A, File S1). Furthermore, to leading order, the second moment of change in allele frequency is equal to the neutral case and can be derived in the diffusion limit ($N_{tot} \to \infty$).

Given a single variable, p_{ave}, changing slowly over evolutionary time, we can then use standard diffusion methods to calculate the fixation probability of a mutation in a haploid-diploid population, $u(p_0^{Model})$, where "*Model*" is *G* for global and *L* for local (considered

167 in the next section). The diffusion is a function of the first and second moments of change in the
168 mutant allele frequency, $m^{Model}(p_{ave})$ and $v^{Model}(p_{ave})$, both measured in time units of N_{tot}
169 generations:

$$u\left(p_0^{Model}\right) = \frac{\int_0^{p_0^{Model}} \exp[-2Q^{Model}(p')]\,dp'}{\int_0^1 \exp[-2Q^{Model}(p')]\,dp'}, \tag{3a}$$

$$m^{Model}(p_{ave}) = \frac{N_{tot}p_{ave}(1-p_{ave})}{2}\left[2s_{ave}^{Model} + 2c_D^{Model}p_{ave}(1-2h)s_{MM}^{w}\right], \tag{3b}$$

$$v^{Model}(p_{ave}) = \frac{p_{ave}(1-p_{ave})\left[\left(c_D^{Model}\right)^2\hat{\rho}_H^{Model} + \left(c_H^{Model}\right)^2\left(2\hat{\rho}_D^{Model}\right)\right]}{\hat{\rho}_H^{Model}\left(2\hat{\rho}_D^{Model}\right)}. \tag{3c}$$

170 where p_0^{Model} is the initial allele frequency of mutants (we focus on the case with a single initial
171 mutant allele, $p_0^{Model} = 1/\left[N_{tot}\left(\hat{\rho}_H^{Model} + 2\hat{\rho}_D^{Model}\right)\right]$) and
172 $Q^{Model}(p) = \int(m^{Model}(p)/v^{Model}(p))dp$. For the global regulation model, the average
173 selection acting upon rare mutant alleles across haploid and diploid stages, s_{ave}^{G}, can be
174 calculated from the first moment equation (Appendix 1) and equals:

$$s_{ave}^{Model} = c_H^{Model}s_M^w + c_D^{Model}s_{RM}^w + \phi^{Model}c_D^{Model}\frac{s_M^f}{2}, \tag{4a}$$

$$\phi^{Model} = \frac{(1-a_H)\tilde{w}_R\hat{\rho}_H^{Model}}{(1-a_H)\tilde{w}_R\hat{\rho}_H^{Model} + a_D w_{RR}\hat{\rho}_D^{Model}}. \tag{4b}$$

175 where $\tilde{w}_R = f_R w_R/2$ is the fitness of haploids considering the cost of sex. As we will see later,
176 this equation is valid for local regulation model. The term ϕ^{Model} indicates the fraction of the
177 diploids in the next generation that come from the union of gametes rather than diploid asexual
178 reproduction. With obligately sexual haploid-diploids ($a_H = a_D = 0$, where $c_H^{Model} = c_D^{Model} =$
179 $1/2$ and $\phi^{Model} = 1$), these results coincide with those of Bessho and Otto (2017).
180
181 3.2. Fixation probability in the local regulation model
182 We next derive the fixation probability in a haploid-diploid population when density

dependence regulates haploid and diploid populations separately (Figure 1b), by again applying a transformation of variables and separation of time scales. For the local regulation model, the appropriate weights for the average allele frequency are similar to the global regulation model, where now the class reproductive values, expressed as proportions, are:

$$c_H^L = \frac{1 + \dfrac{a_H w_R \hat{\rho}_H^L}{(1-a_D) w_{RR} \hat{\rho}_D^L}}{2 + \dfrac{a_H w_R \hat{\rho}_H^L}{(1-a_D) w_{RR} \hat{\rho}_D^L} + \dfrac{2}{f_R} \dfrac{a_D w_{RR} \hat{\rho}_D^L}{(1-a_H) w_R \hat{\rho}_H^L}}, \tag{5a}$$

$$c_D^L = \frac{1 + \dfrac{2}{f_R} \dfrac{a_D w_{RR} \hat{\rho}_D^L}{(1-a_H) w_R \hat{\rho}_H^L}}{2 + \dfrac{a_H w_R \hat{\rho}_H^L}{(1-a_D) w_{RR} \hat{\rho}_D^L} + \dfrac{2}{f_R} \dfrac{a_D w_{RR} \hat{\rho}_D^L}{(1-a_H) w_R \hat{\rho}_H^L}}. \tag{5b}$$

After applying a separation of time scales and conducting a diffusion approximation, we conclude that the solution for the fixation probability in a haploid-diploid population, Eqs. (3), remains valid for the local regulation model (Supplementary *Mathematica* file), with the average selection coefficient now being given by Eqs. (5).

3.3. Effective genetic parameters

Using the first and second moments of change in allele frequency, we derive effective genetic parameters to compare our results to the dynamics found in the classical model for fully haploid or fully diploid organisms (Bessho and Otto 2017). More specifically, we define the effective selection coefficient (s_e), dominance coefficient (h_e), and effective population size (N_e) that would result in the same expected change in allele frequency and variance as in the classical diploid model of selection.

For selection, the diploid model is: $\Delta p_{ave} = s_e p_{ave}(1 - p_{ave})[h_e + (1 - 2h_e)p_{ave}]$ (Crow and Kimura 1970; Bessho and Otto 2017). Because this equation depends on the allele

frequency in the same way as Eq. (3b), we can find the effective and dominance selection coefficient from $\Delta p_{ave}/[p_{ave}(1-p_{ave})] = s_e h_e$ when $p_{ave} = 0$ and $\Delta p_{ave}/[p_{ave}(1-p_{ave})] = s_e(1-h_e)$ when $p_{ave} = 1$, yielding:

$$s_e^{Model} = 2s_{ave}^{Model} + 2\hat{c}_D^{Model}\frac{(1-2h)s_{MM}^{w}}{2}. \tag{6a}$$

$$h_e^{Model} = \frac{2s_{ave}^{Model}}{4s_{ave}^{Model} + 2\hat{c}_D^{Model}(1-2h)s_{MM}^{w}}. \tag{6b}$$

When the mutation is additive ($h = 1/2$), these effective parameters are $s_e^{Model} = 2s_{ave}^{Model}$ and $h_e^{Model} = 1/2$.

We next derive the variance effective population size by equating the one generation change in variance (Eq. 3c divided by the time scale, N_{tot}) to the variance in allele frequency expected in the classical Wright-Fisher model, $p_{ave}(1-p_{ave})/2N_e$ with N_e diploid individuals, obtaining:

$$N_e^{Model} = \frac{p_{ave}(1-p_{ave})}{2(v^{Model}/N_{tot})} = \frac{N_{tot}\,\hat{\rho}_H^{Model}\hat{\rho}_D^{Model}}{\left(c_D^{Model}\right)^2\hat{\rho}_H^{Model} + 2\left(c_H^{Model}\right)^2\hat{\rho}_D^{Model}}. \tag{7}$$

Plugging these effective parameters into the formula from the fixation probability in the classical diploid Wright-Fisher model (Kimura 1957; 1962; Crow and Kimura 1970, p. 427), the fixation probability in a haploid-diploid population given by Eq. 3a can be expressed as:

$$u(p_0^{Model}) = \frac{\int_0^{p_0^{Model}} \exp[-2N_e^{Model}s_e^{Model}\{(2h_e^{Model}-1)p'(1-p') + p'\}]\,dp'}{\int_0^1 \exp[-2N_e^{Model}s_e^{Model}\{(2h_e^{Model}-1)p'(1-p') + p'\}]\,dp'}. \tag{8}$$

Assuming an initially rare and additive mutation ($h = 1/2$) with weak positive selection in a large population ($s_e^{Model}N_e^{Model}p_0^{Model} \approx 0$ and $s_e^{Model}N_e^{Model} \gg 1$), we obtain the classic approximation, $u\left(p_0^{Model}\right) \approx 2s_e^{Model}N_e^{Model}p_0^{Model}$, which upon substituting from Eq. 7 yields:

$$u(p_0^{Model}) \approx \frac{2\hat{\rho}_H^{Model}\hat{\rho}_D^{Model}}{(\hat{\rho}_H^{Model} + 2\hat{\rho}_D^{Model})\left[\left(c_D^{Model}\right)^2\hat{\rho}_H^{Model} + 2\left(c_H^{Model}\right)^2\hat{\rho}_D^{Model}\right]}2s_{ave}^{Model}. \tag{9a}$$

For example, because haploids and diploids have the same reproductive values in the obligately sexual case ($\hat{c}_H^{Model} = \hat{c}_D^{Model} = 1/2$), we obtain:

$$u\left(p_0^{Model}\right) \approx \frac{8\hat{\rho}_H^{Model}\hat{\rho}_D^{Model}}{\left(\hat{\rho}_H^{Model} + 2\hat{\rho}_D^{Model}\right)^2}\, 2s_{ave}^{Model} \tag{9b}$$

(Eq. 13a in Bessho and Otto 2017), or simply $u\left(p_0^{Model}\right) \approx 2s_{ave}^{Model}$ if haploid and diploid population sizes are equal in terms of number of chromosomes ($\hat{\rho}_H^{Model} = 2/3$).

In the next three sections, we explore the implications of these results for the evolution of haploid-diploid populations.

3.4. Effective selection in a haploid-diploid population

The strength of selection averaged across haploids and diploids, s_{ave}^{Model}, plays a key role in the evolution of haploid-diploid populations. When a mutation is rare, both the rate of change in allele frequency (Eq. 3b) and the approximate fixation probability (Eq. 10a) are proportional to s_{ave}^{Model}. We thus begin by exploring how s_{ave}^{Model} varies as we alter the amount of asexual reproduction in haploid and diploid phases. We focus on the case where the mutation does not affect fertilization success ($s_M^f = 0$), so that the average selection becomes:

$$s_{ave}^{Model} = c_H^{Model} s_M^w + c_D^{Model} s_{RM}^w, \tag{10}$$

in both global and local regulation models (Eqs. (4) and (6)).

The relative evolutionary importance of selection in the haploid and diploid phases is thus determined by the class reproductive values, c_H^{Model} and c_D^{Model} (where $c_H^{Model} + c_D^{Model}$=1). Figures 2 (global regulation) and 3 (local regulation) illustrate the proportional reproductive value of haploids, c_H^{Model}, as a function of the degree of asexual reproduction in haploids (x-axis) and diploids (ranging from 0.05 in red to 0.95 in blue). With global regulation, the frequency of haploidy within the population, $\hat{\rho}_H^G$ (given by Eq. A.4), varies with the parameters (see inset graphs in Figure 2), rising with the frequency of haploid asexuality (x-axis in inset) but declining with more asexuality in diploids (from red to blue). By contrast, with local

regulation, the frequency of haploidy is held fixed by the strict density dependent competition that we have assumed ($\hat{\rho}_H^L = 0.8$ in Figure 3(a)(b) and 0.3 in 3(c)(d)).

In the left panels, haploids have a higher fertility ($w_R/w_{RR} = 5$), leading to a higher haploid reproductive value, c_H^{Model}, especially with local regulation when haploids are also more common ($\hat{\rho}_H^L = 0.8$ in Figure 3a). In the right panels, diploids have a higher fertility ($w_{RR}/w_R = 5$), leading to a lower haploid reproductive value, especially when haploids are rare ($\hat{\rho}_H^L = 0.3$ in Figure 3d).

When haploids are primarily sexual ($a_H \approx 0$), increasing asexuality of the haploid stage typically causes the reproductive value of haploids to rise, unless diploids are fitter and more frequent (Figure 3d and blue curves in Figure 2b). At the other extreme, the reproductive value of haploids typically plummets to zero as haploid reproduction becomes primarily asexual ($a_H \approx 1$) while diploids remain sexual, particularly with local regulation (Figure 3), because haploids then act as a genetic "sink" contributing little to the diploid sub-population. This downward trend when haploids are predominantly asexual is also seen with global regulation if diploids are more fit (Figure 2b), except when the diploid population does not sustain itself and goes extinct, which occurs when $a_D < 0.2$ and $a_H = 1$. The net result can thus be non-monotonic (purple curves with $0.2 < a_D < 0.4$ in Figure 2b and Figure 3(a)(b)(c)).

3.4. Effective population size in a haploid-diploid population

We next consider the effective size of haploid-diploid populations with varying degrees of asexuality. Figure 4 plots the effective population size (Eq. 8) relative to the total population size, N_e^{Model}/N_{tot}, as a function of the frequency of haploids, $\hat{\rho}_H^{Model}$ (x-axis), and the class reproductive values (with c_H^{Model} ranging from 0.05 in blue to 0.95 in red). As noted by Bessho and Otto (2017), the effective population size is highest – and drift weakest – at intermediate

frequencies of haploids and diploids, which ensures the least sampling error as organisms alternate generations.

When haploids and diploids have equal reproductive values, as in the fully sexual case ($c_H^{Model} = c_D^{Model} = 1/2$), the effective population size is maximized at $\hat{\rho}_H^{Model} \approx 0.586$. With asexual reproduction, the peak shifts towards whichever ploidy level has the higher reproductive value. For example, if haploids have a high reproductive value (red) then the effective population size is maximized at a higher frequency of haploids, reducing the amount of genetic drift in that phase. Although not illustrated, the peak shifts to $N_e^{Model} = \hat{\rho}_D^{Model} N_{tot}$ when future populations descend only from diploids ($c_H^{Model} = 0$) and to $N_e^{Model} = \left(\hat{\rho}_H^{Model}/2\right) N_{tot}$ when future populations descend only from haploids ($c_H^{Model} = 1$), effectively becoming diplontic or haplontic, respectively (with the $1/2$ arising because haploids have half the number of chromosomes).

Of course, the reproductive values, as well as the frequency of haploids with global population regulation ($\hat{\rho}_H^G$), depend in turn on the fitness parameters and the extent of asexuality, as explored in the previous section. Figures 5 (global regulation) and 6 (local regulation) illustrate the effective population size as a function of the frequency of haploid asexuality, a_H (x-axis), and the frequency of diploid asexuality (a_D rising from red to blue), using the parameters in Figures 2 and 3, respectively. The trends are often non-monotonic, with N_e^{Model}/N_{tot} values varying around $1/2$ when the parameter values are intermediate. The effective population size is often higher when diploids rarely reproduce asexually (red) rather than when they frequently do (blue), although there are exceptions (particularly when the fitness and frequency of diploids is high).

3.6. Fixation probability in a haploid-diploid population

We next compare the above results with numerical simulations estimating the fixation probability of a newly arisen mutation in a haploid-diploid population. When simulating the global regulation model, we assumed that the population has reached the demographic equilibrium, $\hat{\rho}_H^G N_{tot}$ haploids and $\hat{\rho}_D^G N_{tot}$ diploids (see Appendix A). We then chose one resident allele *R* at random and replaced it with a mutant allele *M*. After mutation, offspring were sampled from the parental generation according to a multinomial distribution with expected frequencies given by $x_{(GT)}$, repeating until the mutant allele fixed or was lost from the population. We estimated the fixation probability as the fraction of 10,000 replicate simulations leading to fixation.

We here consider the additive case ($h = 1/2$ and $h_e = 1/2$), where the fixation probability (Eq. 8) simplifies to:

$$u\left(p_0^{Model}\right) = \frac{\exp[-2p_0^{Model} N_e^{Model} s_e^{Model}] - 1}{\exp[-2N_e^{Model} s_e^{Model}] - 1} \qquad (11)$$

and where $s_e^{Model} = 2\, s_{ave}^{Model}$ (Eq. 6). Figure 7 plots the fixation probability as a function of the average selection pressure, s_{ave}^{Model}, when the reproductive values and chromosome numbers in haploids and diploids are equal ($c_H^{Model} = c_D^{Model}$ and $\hat{\rho}_H^{Model} = 2/3$) and $s_{ave}^{Model} = [(1/2sMw+1/2sRMw$. The diffusion Eq. (11) provides an excellent fit, as does the approximation Eq. (9b) for selection coefficients that are positive and not too weak. In this case, the results are the same with global and local population regulation (Fig. 7a and 7b, respectively) and are insensitive to how much selection occurs in the haploid or diploid phases (s_M^{Model} and s_{RM}^{Model}, respectively), as long as s_{ave}^{Model} is held constant (see additional simulations in Supplementary *Mathematica* file). As expected, the extent of selection in the haploid versus diploid phase matters more when the mutation is not additive ($h \neq 1/2$ and $h_e \neq 1/2$) (supplementary *Mathematica* file).

Next, we illustrate the approximate fixation probability, Eq. (9a), as a function of the

311 degree of asexuality (a_H and a_D) when the population size is globally (Fig. 8) or locally (Fig. 9)
312 regulated, assuming only selection in haploids or only in diploids. For example, with additive
313 mutations, the fixation probability can be approximated as $u \approx 4c_H^{Model} N_e^{Model} p_0^{Model} s_M^w$ when
314 selection occurs only in the haploid phase or $u \approx 4c_D^{Model} N_e^{Model} p_0^{Model} s_{RM}^w$ with selection only
315 in the diploid phase, indicating that the fate of mutations depends as much on the strength of
316 selection as on the reproductive value of the ploidy phase in which selection acts (as illustrated in
317 Fig. 2 and 3). Figures 8 (global) and 9 (local) illustrate how the fixation probability depends on
318 the various parameters in the model, particularly the amount of asexual reproduction in haploids
319 (x-axis) and diploids (a_D rising from red to blue). The trends can be understood by the combined
320 effects of the parameters on the reproductive value and the effective population size (e.g., Fig.
321 9(a) is proportional to the product of Fig. 3(a) and Fig. 6(c)).
322
323 **4. Discussion**
324 Across the phylogenetic tree of life, organisms have diverse and complex reproductive
325 strategies (Bell 1982). Classical population genetic theory has, however, focused most on fully
326 haploid or diploid life cycles with obligate sexuality. In this article we develop a stochastic
327 model for the population genetics of haploid-diploid organisms considering demography,
328 asexuality, and habitat differentiation between haploid and diploid stages. Using a separation of
329 time scales, we derive a diffusion approximation for the change in allele frequency, allowing us
330 to estimate the fixation probability of new mutations, the effective strengths of selection and
331 dominance, as well as the effective population size of haploid-diploid populations.
332
333 5.1. Natural selection in a haploid-diploid population
334 Our results indicate that the strength of natural selection and the extent of genetic drift

depend strongly on the reproductive value of haploid versus diploid phases. In the simplest case, when the effect of a mutation is weak, additive, positive, and absent in the gamete stage ($s_M^f = 0$), the fixation probability is proportional to the effective strength of selection (Eq. 10), $s_e^{Model} = 2s_{ave}^{Model}$, which in turn is proportional to the amount of selection in and the reproductive value of haploids and diploids (Eqs. 2, and 5).

These analytical results reveal some evolutionary principles for populations that undergo an alternation of generations. One consequence is that the balance of opposing selection pressures in haploids and diploids (Eqs. 4 and 6) depends not only on the selection coefficients, but also on the relative reproductive values of haploids (c_H^{Model}) versus diploids (c_D^{Model}). Thus, the very direction of evolution depends on the extent of asexuality in the two phases and the relative survival and fertility of haploids versus diploids when there is "ploidally antagonistic selection" (Immler et al. 2012).

The efficacy of selection to fine tune traits in haploids and diploids also depends on the class reproductive values. For example, when the population is regulated by local density dependence (i.e., the haploid and diploid phases are spatially or temporally distinct), higher reproductive success in haploids increases the efficiency of haploid selection (compare Figure 3a to 3b). However, when there is extremely rare sexuality in haploids (a_H near one), diploid selection tends to be more effective because of increasing competition between offspring from haploids. By contrast, the trends differ with global density dependence (e.g., species that are more isomorphic with small ecological differences between stages). For example, the reproductive value of haploids remains high even when they reproduce primarily asexually in the global regulation model (see Figure 2 when a_H approaches one), because haploids then make up a larger proportion of the total population size (see inset figures). Thus, whether selection is effective in the haploid phase when that phase mainly reproduces asexually is quite sensitive to

359 the nature of competition.

360 Our work can also be useful in the design of field studies and the interpretation of data
361 for species that alternate generations. To understand the efficiency of selection on haploid and
362 diploid phases, we not only need data about the fraction of haploids and diploids and their
363 fertility and mortality (e.g., Thornber and Gains 2004; Vieira et al., 2018a; Vieira et al. 2018b),
364 but we also need to know about the extent of asexuality in each phase and whether they compete
365 for common or different resources.

366

367 5.2. Genetic drift and effective size

368 The impact of random genetic drift on the genetic diversity of haploid-diploid
369 population depends on the effective population size (Eq. 7). As we had found previously in a
370 haploid-diploid model with obligate sexuality (Bessho and Otto 2017, pp. 431), the effective
371 population size with asexuality is generally smaller than the total number of individuals and
372 again depends strongly on the reproductive value of each phase (Figures 4-6). With obligate
373 sexuality, the reproductive values of haploids and diploids are equal, and the effective population
374 size is maximized (drift minimized) when haploids comprise 2/3 of the population, making the
375 number of chromosomes equal between haploids and diploids. Asexual reproduction, however,
376 causes the reproductive value of haploids and diploids to differ (Eqs. 2 and 5). Consequently,
377 drift is lessened if the phase with the higher reproductive value is more common (see shifts in
378 peaks in Figure 4).

379

380 5.3. "Ploidally-structured" population

381 The key role that reproductive values play in this work is analogous to the role that
382 patch dynamics play in two-patch models of evolution. In a spatially structured population,

subdivided local populations are genetically connected by migration. A haploid-diploid system can be seen as being ploidally structured, where gene flow describes the movement of alleles through sexual reproduction, with meiosis causing flow to haploidy and syngamy flow to diploidy. We note that our research reveals that all qualitative results are equally accurate for evolution in a two-patch system (see Supplementary *Mathematica* File). For example, fixation probability strongly depends on class reproductive values of each patch.

This analogy suggests an interesting idea: complex reproductive systems can be considered and analyzed using the tools of metapopulation theory. For example, many eukaryotes including terrestrial plants, insects, and fishes, often exhibit ploidy variation, including polyploid members (Otto and Whitton 2000; Comai 2005). In such species, individuals characterized by different numbers of chromosomes coexist, with complex reproductive relationships causing gene flow between them (Ramsey and Schemske 1998). Similarly, social insects often exhibit complex sex determination systems linked with ploidy levels (haplodiploidy).

Our research suggests that these ploidally-structured populations can be fruitfully treated as metapopulations. Selection and drift in populations with diploids, triploids, and tetraploids can, for example, be considered as a three-patch model. In this system, we conjecture that the average strength of selection that is evolutionarily relevant would be the mean selection coefficient in each ploidy class, weighted by its class reproductive value, with additional terms coming from reproductive interactions (akin to the term of s_M^f in Eqs. 4).

Many evolutionary aspects of haploid-diploid populations remain to be investigated. One avenue that we are exploring is how model parameters can be estimated from field data. For example, the analogy between spatially and ploidally structured population suggests that genetic differences between haploids and diploid can be used to estimate gene flow between them (i.e.,

rates of sex), akin to using Fst to inform estimates of migration (e.g., Slatkin 1987). Another fruitful avenue for further work is to determine how fluctuations in population size affect the effective population size of species that alternate generations. In classical population genetics theory, such fluctuations can be captured by using the harmonic mean population in place of the total population size (Karlin 1968). It is unclear, however, whether the same is true in haploid-diploid populations. Can the harmonic total population size simply replace N_{tot} in the global model of population regulation? Similarly, can the harmonic population sizes of haploids and diploids replace N_H and N_D with local regulation? The answer is unclear because population size fluctuations perturb the fast ecological dynamics away from the steady state (especially $\hat{\rho}_H^{Model}$), and the impact of these perturbations on selection and drift is unknown. Further research is needed to clarify evolutionary processes in the wide variety of species that alternate generations.

Acknowledgements

We here thank Alireza Ghaseminejad for help in developing our manuscript. We also thank H. Ohtsuki and Y. Uchiumi for the helpful comment.

Funding sources

This project was funded by a Grand-in-Aid from a Japan Society for the Promotion of Science (JSPS) to KB (16J05204) and by a Discovery grant from the Natural Sciences and Engineering Research Council of Canada (NSERC RGPIN-2016-03711) to S.P.O.

Appendix A. Fixation probability in a haploid-diploid Wright-Fisher model using a diffusion approximation

A.1. Equilibrium with global regulation

We derive the fixation probability in a haploid-diploid population using a diffusion approximation (e.g., Bessho and Otto 2017). We first derive the stable equilibrium in the global regulation model, allowing for asexual reproduction in each phase. In the Wright-Fisher model, all individuals reproduce and then the parents die (non-overlapping generations). Let $b_{(GT)}$ represent the number of reproductive cells of each type in the next generation:

$$b_R = (1-a_D)w_{RR}x_{RR} + (1-a_D)\frac{w_{RM}x_{RM}}{2} + a_H w_R x_R, \tag{A.1a}$$

$$b_M = (1-a_D)\frac{w_{RM}x_{RM}}{2} + (1-a_D)w_{MM}x_{MM} + a_H w_M x_M, \tag{A.1b}$$

$$b_{RR} = (1-a_H)\frac{f_R}{2}\frac{w_R^2 x_R^2}{w_R x_R + w_M x_M} + a_D w_{RR} x_{RR}, \tag{A.1c}$$

$$b_{RM} = (1-a_H)\frac{f_R + f_M}{2}\frac{w_R w_M x_R x_M}{w_R x_R + w_M x_M} + a_D w_{RM} x_{RM}, \tag{A.1d}$$

$$b_{MM} = (1-a_H)\frac{f_M}{2}\frac{w_M^2 x_M^2}{w_R x_R + w_M x_M} + a_D w_{MM} x_{MM}. \tag{A.1e}$$

The probability that a reproductive cell of genotype (*GT*) is sampled from the offspring produced by the previous generation of adults is

$$q_{(GT)} = \frac{b_{(GT)}}{b_R + b_M + b_{RR} + b_{RM} + b_{MM}}. \tag{A.2}$$

Therefore, the composition of offspring in the next generation is given by the multinomial distribution, sampling N_{tot} individuals in proportion to Eq. (A2). Using Eq. (A1) and (A2), we describe the conditional expectation of change in the number of individuals of genotype (*GT*), $\Delta X_{(GT)}(t) = X_{(GT)}(t+1) - X_{(GT)}(t)$, as

$$\mathrm{E}\left[\Delta X_{(GT)}(t) | \vec{X}(t) = \vec{x}\right] = N_{tot} q_{(GT)} - x_{(GT)}, \tag{A.3}$$

where $\mathrm{E}\left[\Delta F\left(X_{(GT)}(t)\right)|\vec{X}(t)=\vec{x}\right]$ is the conditional expected value for change in the function F of the random variable given that $\vec{X}(t)=(X_R(t) \quad X_M(t) \quad X_{RR}(t) \quad X_{RM}(t) \quad X_{MM}(t))^T$ equals $\vec{x}=(x_R \quad x_M \quad x_{RR} \quad x_{RM} \quad x_{MM})^T$.

To simplify this fully stochastic system, we assume that the resident population is large and treat demographic changes deterministically prior to the appearance of the mutation. Considering the dynamics of the resident population, we then find the equilibrium of these dynamical equations by solving $N_{tot}q_R-\hat{x}_R=0$ and $N_{tot}q_{RR}-\hat{x}_{RR}=0$ ($\hat{x}_R+\hat{x}_{RR}=N_{tot}$). Setting $\hat{x}_R=\hat{\rho}_H^G N_{tot}$ and $\hat{x}_{RR}=\hat{\rho}_D^G N_{tot}$, the fraction of haploids $\hat{\rho}_H^G$ (and diploids $\hat{\rho}_D^G=1-\hat{\rho}_H^G$) at equilibrium becomes,

$$\hat{\rho}_H^G=\frac{a_H w_R+a_D w_{RR}-2w_{RR}+\sqrt{4(1-a_H)(1-a_D)\tilde{w}_R w_{RR}+(a_H w_R-a_D w_{RR})^2}}{2[a_H w_R+(1-a_H)\tilde{w}_R-w_{RR}]}, \qquad \text{(A.4)}$$

where $\tilde{w}_R=f_R w_R/2$ is the fitness of haploids considering the cost of sex (see Supplementary *Mathematica* file for the step-by-step derivation). We note that, when the fertility of haploids is much greater than that of diploids ($w_R \gg w_{RR}$), the frequency of haploids in a population approaches $a_H/\{a_H+[(1-a_H)f_R/2]\}$, which is less than one because sexual reproduction of the haploids produces diploids (the $(1-a_H)f_R/2$ term). Conversely, when the fertility of diploids is much greater than haploids ($w_R \ll w_{RR}$), the frequency of haploids approaches $1-a_D$, the rate at which diploids undergo meiosis.

A.2. First moment of change in allele frequency

To derive the first moment of change in allele frequency, $m^{Model}(p_{ave})$, we apply a separation of time scales (e.g., Nagylaki 1976; Otto and Day 2007; Bessho and Otto 2017). Details of the calculation are represented in the Supplementary *Mathematica* file. We first transform the expected change in the number of individuals of each type (five variables that sum

to N_{tot}) into the expected change in a new set of four variables, $\Theta \in \{p_{ave}, \delta_p, \eta_{HW}, \rho_H\}$, described by the functions:

$$\mathrm{E}\left[\Delta\Theta \,|\, \vec{X}(t) = \vec{x}\right] = f_{\Theta}^{Model}\left(\epsilon, p_{ave}, \vec{\theta}\right), \tag{A.5}$$

where $\vec{\theta} = \left(\delta_p, \eta_{HW}, \rho_H\right)$ and ϵ is proportional to the selection coefficients and assumed small (the functions *f* are given explicitly in the Supplementary *Mathematica* file). With local regulation, ρ_H is assumed fixed at N_H/N_{tot} and dropped from the variable set, Θ.

To constant order (setting the small changes due to selection to zero, $\epsilon \to 0$), the fast ecological dynamics of the system are described by: $f_{\Theta}^{Model}\left(0, p_{ave}, \vec{\theta}\right)$. This system of equations rapidly approaches a steady state found by solving $f_{\Theta}^{Model}\left(0, p_{ave}, \vec{\theta}\right) = 0$, which gives $\bar{\delta}_p = \bar{\eta}_{HW} = 0$, and $\bar{\rho}_H = \hat{\rho}_H^G$ (Eq. A.4). To this order, the steady state change in allele frequency is zero, $f_{p_{ave}}^{Model}\left(0, p_{ave}, \vec{\theta}\right) = 0$. We then describe slower changes, including changes in allele frequency due to selection, by describing the deviations that occur around this steady state. Specifically, to order ϵ, the variables are allowed to deviate from the steady state by $\delta_p = \tilde{\delta}_p\epsilon$, $\eta_{HW} = \tilde{\eta}_{HW}\epsilon$, and $\rho_H = \hat{\rho}_H^G + \tilde{\rho}_H\epsilon$, and the dynamics $f_{\Theta}^{Model}\left(\epsilon, p_{ave}, \vec{\theta}\right)$ are then approximated using a Taylor series expansion. Defining the average allele frequency by combining haploid and diploid populations using an arbitrary weighting, $p_{ave} = \omega p_H + (1-\omega)p_D$, we show in the Supplementary *Mathematica* file that setting the weights proportional to the class reproductive values (given by Eq. (2) with global regulation and Eq. (5) with local regulation) is the only choice that separates evolutionary change in p_{ave} from changes in the other variables to order ϵ. Defining the average allele frequency in this way (Eq. 1a) and taking the Taylor series, the change in allele frequency becomes:

$$\mathrm{E}\left[\Delta p_{ave} \,|\, \vec{X}(t) = \vec{x}\right] \approx M^{Model}(p_{ave}) \tag{A.6}$$

$$= \frac{p_{ave}(1-p_{ave})}{2}\left[2s_{ave}^{Model} + 2c_D^{Model}p_{ave}(1-2h)s_{MM}^{w}\right].$$

485

486 A.3. Second moment of change in average allele frequency

487 We next derive the second moment of change in average allele frequency in a
488 haploid-diploid population with asexuality. We again assume that the population size is very
489 large, that selection is very weak, and that the system has approached the steady state in
490 $(\delta_p, \eta_{HW}, \rho_H)$, ignoring deviations that are of $0(\epsilon)$. Because selection is assumed weak, the
491 second moment is well approximated by that of the neutral model (to constant order, $\epsilon \to 0$).

492 Under these assumptions, the fraction of haploids in a population is relatively fixed in
493 both the global and local regulation models, and we can sample the haploid offspring according
494 to a binomial distribution, with expectation and variance: $\mathrm{E}[X_M|\vec{X}(t) = \vec{x}] = q_M N_H$ and
495 $\mathrm{Var}[X_M|\vec{X}(t) = \vec{x}] = q_M(1 - q_M)N_H$ where $q_M = b_M/(b_R + b_M)$. To simplify the equation, we
496 set $\mathrm{E}[X_{(GT)}|\vec{X}(t) = \vec{x}] = m_{(GT)}$ and $\mathrm{Var}[X_{(GT)}|\vec{X}(t) = \vec{x}] = v_{(GT)}$, finding that:

$$\mathrm{E}[\Delta X_M|\vec{X}(t) = \vec{x}] = m_M - x_M, \tag{A.7a}$$

$$\mathrm{E}[(\Delta X_M)^2|\vec{X}(t) = \vec{x}] = v_M + m_M^2 - 2m_M x_M + x_M^2. \tag{A.7b}$$

497 In terms of allele frequencies (rather than numbers), we have the first and second moments for
498 the haploid offspring population, $\mathrm{E}\left[\frac{\Delta X_M}{N_H}|\vec{X}(t) = \vec{x}\right] = \frac{1}{N_H}\mathrm{E}[\Delta X_M|\vec{X}(t) = \vec{x}]$ and
499 $\mathrm{E}\left[\left(\frac{\Delta X_M}{N_H}\right)^2|\vec{X}(t) = \vec{x}\right] = \frac{1}{N_H^2}\mathrm{E}[(\Delta X_M)^2|\vec{X}(t) = \vec{x}]$.

500 Similarly, the diploid offspring are sampled according to a trinomial distribution, with
501 expectation, variance, and covariance: $m_{(GT)} = q_{(GT)}N_D$, $v_{(GT)} = q_{(GT)}(1 - q_{(GT)})N_D$, and
502 $\mathrm{Cov}[X_{RM}, X_{MM}|\vec{X}(t) = \vec{x}] = q_{RM}q_{MM}N_D$, where $q_{(GT)} = b_{(GT)}/(b_{RR} + b_{RM} + b_{MM})$. To derive
503 the moments of the allele frequency in diploids, we define, $y_M = (x_{RM}/2) + x_{MM}$ and
504 $Y_M = (X_{RM}/2) + X_{MM}$. The moments of random variable Y are then:

$$\mathrm{E}\left[Y_M|\vec{X}(t)=\vec{x}\right]=\frac{m_{RM}}{2}+m_{MM}, \tag{A.8a}$$

$$\mathrm{E}\left[Y_M^2|\vec{X}(t)=\vec{x}\right]=\frac{v_{RM}+m_{RM}^2}{4}+\left(\mathrm{Cov}\left[X_{RM},X_{MM}|\vec{X}(t)=\vec{x}\right]+m_{RM}m_{MM}\right)+\left(v_{MM}+m_{MM}^2\right), \tag{A.8b}$$

$$\mathrm{E}\left[\Delta Y_M|\vec{X}(t)=\vec{x}\right]=\frac{\mathrm{E}\left[\Delta X_{RM}|\vec{X}(t)=\vec{x}\right]}{2}+\mathrm{E}\left[\Delta X_{MM}|\vec{X}(t)=\vec{x}\right]-y_M, \tag{A.8c}$$

$$\mathrm{E}\left[(\Delta Y_M)^2|\vec{X}(t)=\vec{x}\right]=\mathrm{E}\left[Y_M^2|\vec{X}(t)=\vec{x}\right]-2\mathrm{E}\left[Y_M|\vec{X}(t)=\vec{x}\right]y_M+y_M^2. \tag{A.8d}$$

To consider the change in average allele frequency across the entire population, we define $Z_M=c_H^{Model}\frac{X_M}{N_H}+c_D^{Model}\frac{Y_M}{N_D}$ and consider the expectation of change in this random variable. Plugging in Eqs. (7a), (7b), (8c), and (8d), we have

$$\mathrm{E}\left[(\Delta Z_M)^2|\vec{X}(t)=\vec{x}\right]=\frac{p_{ave}(1-p_{ave})\left[\left(c_D^{Model}\right)^2\hat{\rho}_H^{Model}+\left(c_H^{Model}\right)^2\left(2\hat{\rho}_D^{Model}\right)\right]}{\hat{\rho}_H^{Model}\left(2\hat{\rho}_D^{Model}\right)N_{tot}}. \tag{A.9}$$

After transforming time scales using the variable $\tau=t/N_{tot}$ and defining $P(\tau)=Z(N_{tot}\tau)$, we have the diffusion coefficient $v^{Model}(p_{ave})=\lim_{N_{tot}\to\infty}\mathrm{E}\left[\frac{\left(P(\tau+\Delta\tau)-P(\tau)\right)^2}{\Delta\tau}\right]$ by taking the limit $N_{tot}\to\infty$, giving Eq. (3c). Similarly, we derive the drift coefficient using Eq. (A6) ($m^{Model}=M^{Model}N_{tot}$), giving Eq. (3b).

References

Bell, G. 1982. The Masterpiece of Nature: The Genetics and Evolution of Sexuality. University of California Press. Berkeley, CA.

Bell, G., 1994. The comparative biology of the alternation of generations. Lectures on mathematics in the life sciences 25, 1–26.

Bessho, K., Otto, S. P. 2017. Fixation probability in a haploid-diploid population. Genetics 205, 421-440.

Comai, L. 2005. The advantages and disadvantages of being polyploid. Nature Reviews Genetics 6, 836-846.

Coelho, S. M., Peters, A. F., Charrier, B., Roze, D., Destombe, C., Valero, M., Cock, J. M., 2007. Complex life cycles of multicellular eukaryotes: new approaches based on the use of model organisms. Gene 406, 152–170.

525 Crow, J. F., Kimura, M. (1970). An introduction to population genetics theory. The Blackburn
526 Press, New Jersey.
527 Deithier, M. N. (1981). Heteromorphic algal life histories: The seasonal pattern and response to
528 herbivory of the brown crust, *Ralfsia californica*. Oecologia 49, 333-339.
529 Destombe, C., Godin, J., Nocher, M., Richerd, S., Valero, M. (1993). Differences in response
530 between haploid and diploid isomorphic phases of *Gracilaria verrucosa* (Rhodophyta:
531 Gigartinales) exposed to artificial environmental conditions. Hydrobiologia 260/261,
532 131-137.
533 De Wreede, R. E., Klinger, T. 1988. Reproductive strategies in algae. Plant reproductive ecology:
534 Patterns and strategies, 267-284.
535 Dyck, L. J., De Wreede, R. E. (2006). Seasonal and spatial patterns of population density in the
536 marine macroalga *Mazzaella splendens* (Gigartinales, Rhodophyta). Phycological
537 Research, 54(1), 21-31.
538 Goldstein, D. B. 1992. Heterozygote advantage and the evolution of dominant diploid phase.
539 Genetics 132, 1195–1198.
540 Haghes, J. S., Otto, S. P. 1999. Ecology and the evolution of biphasic life cycles. The American
541 Naturalist 154, 306–330.
542 Hannach, G., Santelicesm, B. 1985. Ecological differences between the isomorphic reproductive
543 phases of two species of *Iridaea* (Rhodophyta: Gigartinales). Marine Ecology Progress
544 Series 22, 291–303.
545 Hawkes, M. W. 1990. Reproductive strategies. Biology of the red algae, 455-476.
546 Immler, S., G. Arnqvist, and S. P. Otto. 2012. Ploidally antagonistic selection maintains stable
547 genetic polymorphism. 66:55–65.
548 Jenkins, C. D., Kirkpatrick, M., 1995. Deleterious mutation and the evolution of genetic life
549 cycles. Evolution, 512–520.
550 Karlin, S. 1968. Rates of approach to homozygosity for finite stochastic models with variable
551 population size. The American Natualist 102, 443-455.
552 Kimura, M., 1957. Some problems of stochastic processes in genetics. The Annals of
553 Mathematical Statistics, 882-901.
554 Kimura, M., 1962. On the probability of fixation of mutant genes in a population. Genetics 47,
555 713.
556 Mable, K. B., Otto, P. S., 1998. The evolution of life cycles with haploid and diploid phases.
557 BioEssays 20, 453–462.
558 Nagylaki, T., 1976. The evolution of one-and two-locus systems. Genetics 83, 583-600.
559 Orr, H. A., Otto, S. P. 1994. Does diploidy increase the rate of adaptation? Genetics 136,
560 1475–1480.

561 Otto, S., Goldstein, D., 1992. Recombination and the evolution of diploidy. Genetics 131,
562 745–751.
563 Otto, S., 1994. The role of deleterious and beneficial mutations in the evolution of ploidy levels.
564 Lectures on Mathematica in the Life Sciences 25, 69–98.
565 Otto, S. P., Marks, J. C. 1996. Mating system and the evolutionary transition between haploidy
566 and diploidy. Biological Journal of the Linnean Society 57, 197-218.
567 Otto, S. P., Day, T., 2007. A biologist's guide to mathematical modeling in ecology and evolution.
568 Princeton University Press.
569 Otto, S. P., Whitton, J. 2000. Polyploid incidence and evolution. Annu. Rev. Genet. 34, 401-437.
570 Perrot, V., Richerd, S., Valéro, M., 1991. Transition from haploidy to diploidy. Nature 351,
571 315–317.
572 Ramsey, J., Schemske, D. W. 1998. Pathways, mechanisms, and rates of polyploid formation in
573 flowering plants. Annual reviews of Ecology and Systematics 29: 467-501.
574 Raper, J. R., Flexer, A. S. (1970). The road to diploidy with emphasis on a detour. In *Symp. Soc.*
575 *Gen. Microbiol* (Vol. 20, pp. 401-432).
576 Rousset, F. (2004). Genetic structure and selection in subdivided populations. Princeton
577 University Press, New Jersey.
578 Scott, M. F., Rescan, M. 2016. Evolution of haploid-diploid life cycles when haploid and diploid
579 fitnesses are not equal. Evolution 71, 215–226.
580 Slatkin, M. 1987. Gene flow and the geographic struture of natural populations. Science New
581 Series 236: 787-792.
582 Slocum C. J. 1980. Differential susceptibility to grazers in two phases of an intertidal alga:
583 Advantages of heteromorphic generations. Journal of Experimental Marine Biology and
584 Ecology 46, 99-110.
585 Taylor, P. D. 1980. Allele-Frequency Change in a Class-Structured Population. The American
586 Naturalist 135, 95-106.
587 Thornber, C. S., Gains, S. D. 2004. Population demographics in species with biphasic life cycle.
588 Ecology 85, 1661-1674.
589 Thornber, C., Stachowicz, J. J., Gains, S. 2006. Tissue type matters: selective herbivory on
590 different life history stages of an isomorphic alga. Ecology 87, 2255-2263.
591 Vieira, V. M. N. C. S., Engelen, A. H., Huanel, O. R., Guillemin, M. 2018a. Haploid females in
592 the isomorphic biphasic life-cycle of *Gracilaria chilensis* excel in survival. BMC
593 Evolutionary Biology 18:174.
594 Vieira, V. M. N. C. S., Engelen, A. H., Huanel, O. R., Guillemin, M. 2018b. Differentiation of
595 haploid and diploid fertilities in *Gracilaria chilensis* affect ploidy ratio. BMC
596 Evolutionary Biology 18:183.

Willson, M. F. 1981. On the evolution of complex life cycles in plants: a review and an ecological perspective. Annals of the Missouri Botanical Garden 68, 275-300.

Figure Captions

Fig. 1. An illustration of the haploid-diploid models. (a) In the global regulation model, both haploids and diploids occupy the same habitat and density dependence holds the total population size N_{tot} constant. (b) In the local regulation model, each ploidy stage occupies a different habit, therefore density dependence regulates the population size of haploids (N_H) and diploids (N_D) separately.

Fig. 2. Class reproductive value of haploids in the global regulation model, c_H^G. Curves show c_H^G as a function of the degree of haploid asexuality, a_H (x-axis), with the degree of diploid asexuality ranging in color from $a_D = 0.05$ (red) to 0.95 (blue) in increments of 0.05. Other parameters are set as: (a) $f_R = 0.5$, $w_R = 5000$, $w_{RR} = 1000$, (b) $f_R = 0.5$, $w_R = 1000$, $w_{RR} = 5000$. The resulting frequency of haploids, $\hat{\rho}_H^G$ (Eq. A.4), is shown in the inset plots.

Fig. 3. Proportional reproductive value of haploids in the local regulation model, c_H^L. Parameters are the same as Fig. 2, except that haploids are held fixed at a frequency of (a)(b) $\hat{\rho}_H^L = 0.8$ or (c)(d) $\hat{\rho}_H^L = 0.3$. We consider the case when (a)(c) haploid fitness parameter is larger than diploid $w_R = 5000$, $w_{RR} = 1000$ ($w_H > w_D$), and when (b)(d) diploid fitness parameter is larger than haploid $w_R = 1000$, $w_{RR} = 5000$ ($w_H < w_D$).

Fig. 4. The effective population size of a haploid-diploid population. The relative effective population size over the total population size (N_e^{Model}/N_{tot}, Eq. 7) is shown as a function of the frequency of haploids ($\hat{\rho}_H^{Model}$, x-axis), when the haploid reproductive value (c_H^{Model}) varies from

622 0.05 (blue) to 0.95 (red) in increments of 0.05. This figure applies to both global and local
623 regulation models.
624
625 Fig. 5. The effective population size of a haploid-diploid population in the global regulation
626 model as a function of the degree of asexuality, a_H and a_D. Parameters are the same as in Fig. 2
627 and determine the relative class reproductive values (c_H^G) and fraction of haploids ($\hat{\rho}_H^G$) according
628 to Eqs. (2a) and (A.4).
629
630 Fig. 6. The effective population size of a haploid-diploid population in the local regulation model.
631 Parameters are the same as in Fig. 3 and determine the relative class reproductive values (c_H^L) by
632 Eqs. (5). The frequencies of haploids are held fixed at a frequency of (a)(b) $\hat{\rho}_H^L = 0.9$, (c)(d)
633 $\hat{\rho}_H^L = 0.8$, (e)(f) $\hat{\rho}_H^L = 0.6$, or (g)(h) $\hat{\rho}_H^L = 0.3$.
634
635 Fig. 7. Fixation probability given the average strength of selection, s_{ave}^{Model}, for global (a) and
636 local (b) regulation models. The solid curve gives the analytical result from the diffusion
637 approximation (Eq. (11)) and the dashed curve gives the linear approximation (Eq. (9b)). Black
638 dots indicate the fixation probability estimated from 10000 numerical simulations with 95% CI
639 (Wilson score interval for binomial). Parameters: $N_{tot} = 90$, $N_H = 60, N_D = 30$, $f_R = 0.5$,
640 $w_R = w_{RR} = 1000$, $a_H = a_D = 0.1$, $h = 0.5$, $s_M^f = 0$, $s_M^w = s_{RM}^w = s_{ave}^{Model}$, such that the
641 fraction of haploids in the resident population is $\hat{\rho}_H^{Model} = 2/3$ and class reproductive values
642 are equal $c_H^{Model} = c_D^{Model} = 1/2$. Holding $s_{ave}^{Model} = 1/2(s_M^w + s_{RM}^w)$ constant, similar results
643 are obtained for a range of different choices of s_M^w and s_{RM}^w (see supplementary *Mathematica*
644 file).
645

Fig. 8. The fixation probability in a haploid-diploid population in the global regulation model. Curves gives the linear approximation for the fixation probability (Eq. (9a)). Parameters are the same as in Fig. 2. Selection acts only in the haploid or diploid phase, with selection coefficients set as $s_M^w = 0.02$ for haploid selection (a)(b) and $s_{RM}^w = 0.02$ for diploid selection (c)(d).

Fig. 9. The fixation probability in a haploid-diploid population in the local regulation model. Curves gives the linear approximation for the fixation probability (Eq. (9a)). Parameters are the same as in Fig. 3 and Fig. 8. The frequency of haploids is held fixed at (a)(b)(e)(f) $\hat{\rho}_H^L = 0.8$, (c)(d)(g)(h) $\hat{\rho}_H^L = 0.3$. Fitness of haploids is higher than diploids in panels (a)(c)(e)(g) ($w_H > w_D$), and the opposite condition is considered in panels (b)(d)(f)(h) ($w_H < w_D$). Selection only occurs in the haploid (a)(b)(c)(d) or diploid stage (e)(f)(g)(h).

Supporting information

S1. Supplementary *Mathematica* file.

Figure1

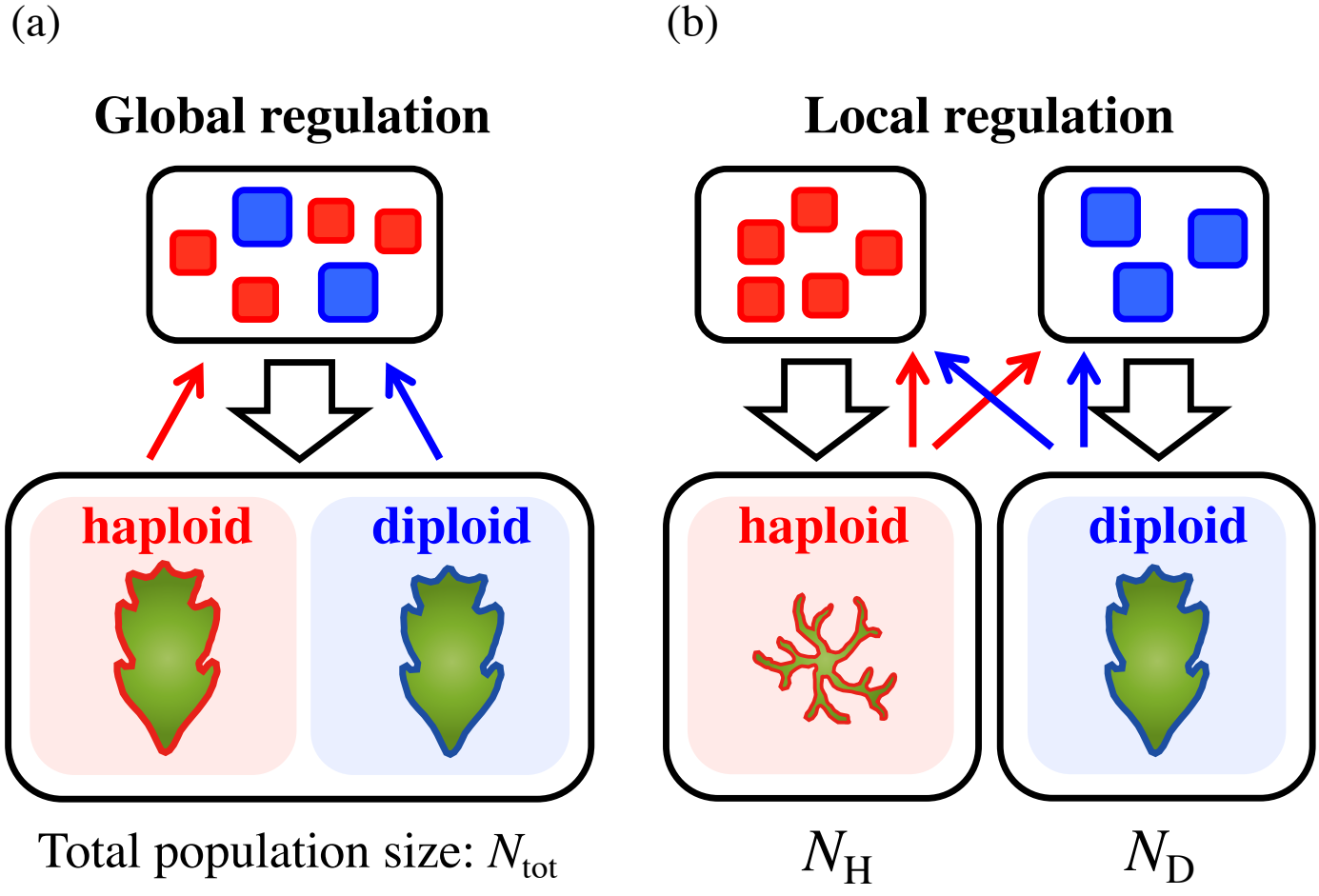
(a)
Global regulation
haploid
diploid
Total population size: N_{tot}
(b)
Local regulation
haploid
diploid
N_H
N_D

Figure 2

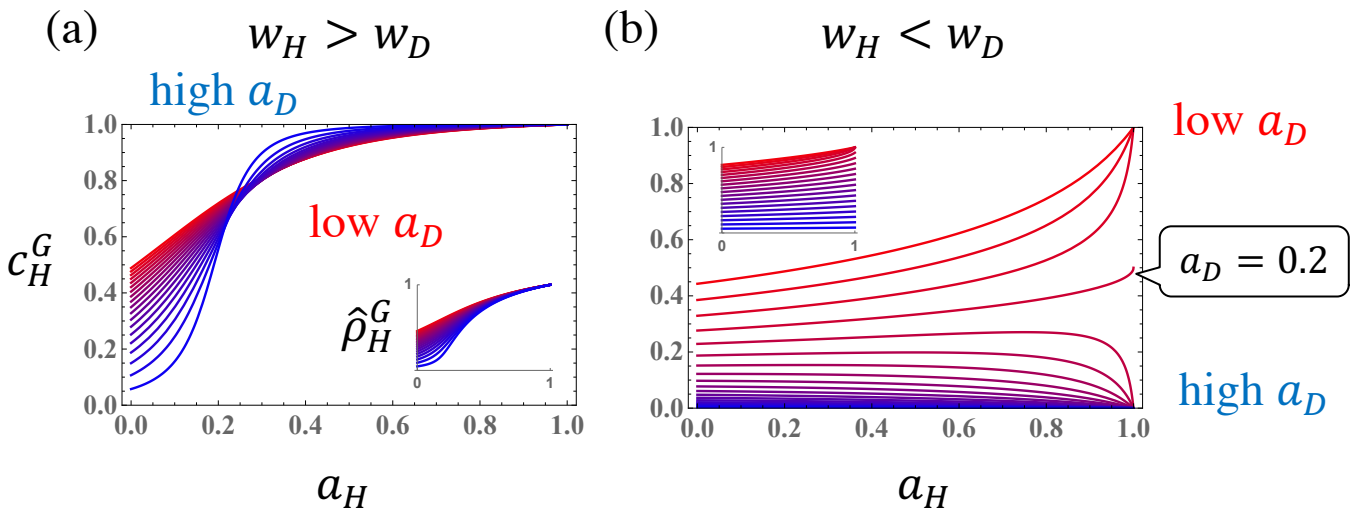
(a)
$w_H > w_D$
high a_D
low a_D
c_H^G
$\hat{\rho}_H^G$
a_H
(b)
$w_H < w_D$
low a_D
$a_D = 0.2$
high a_D
a_H

Figure 3

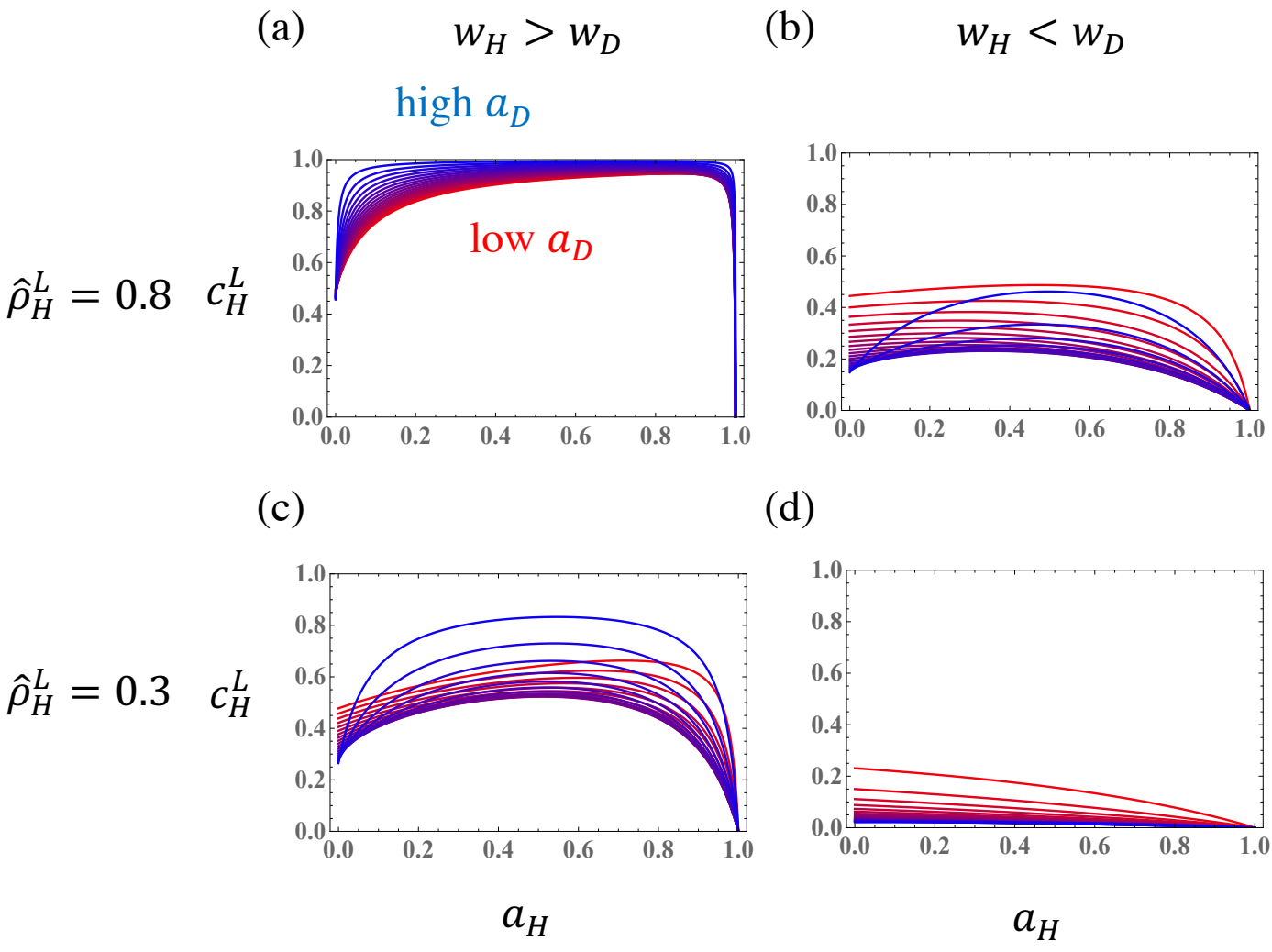

Bessho and Otto

Figure 4

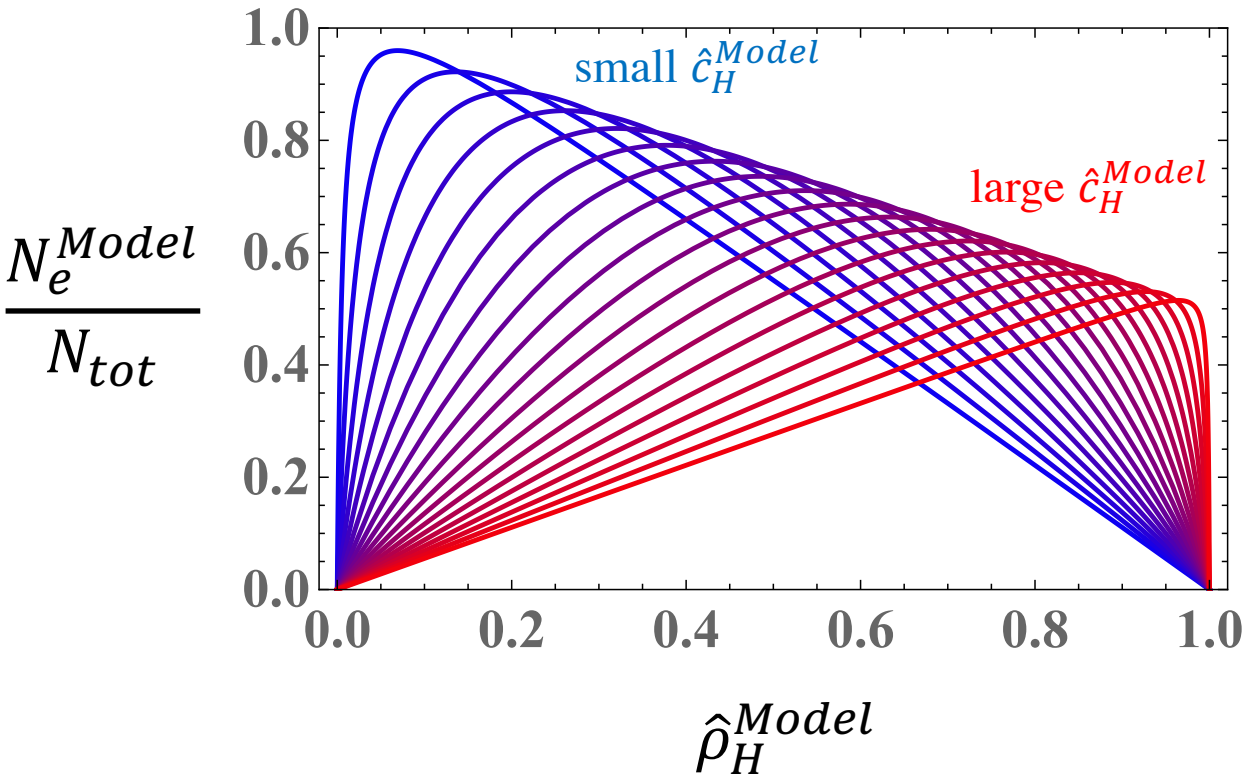

Bessho and Otto

Figure 5

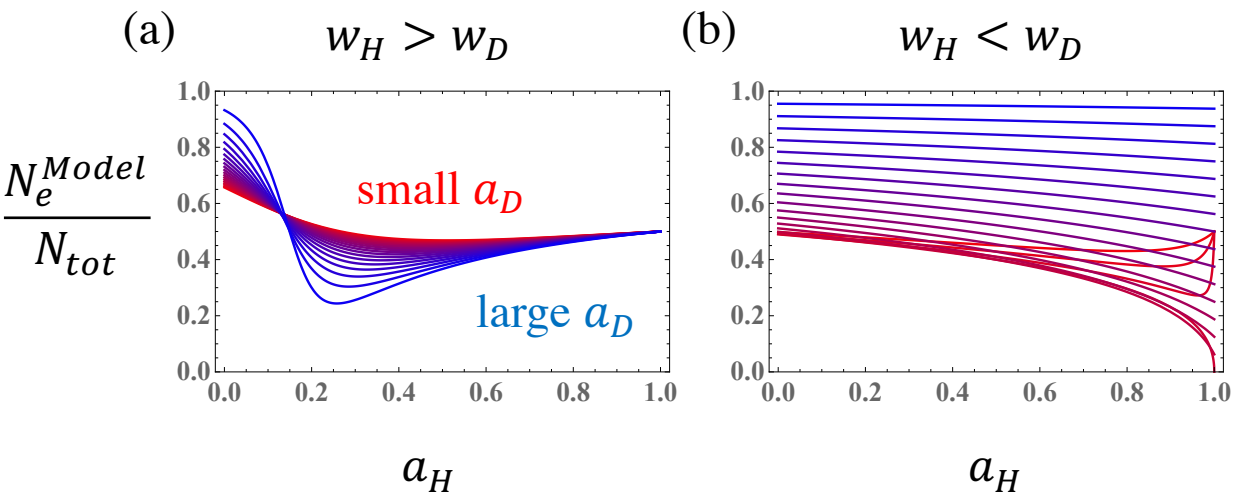

Bessho and Otto

Figure 6

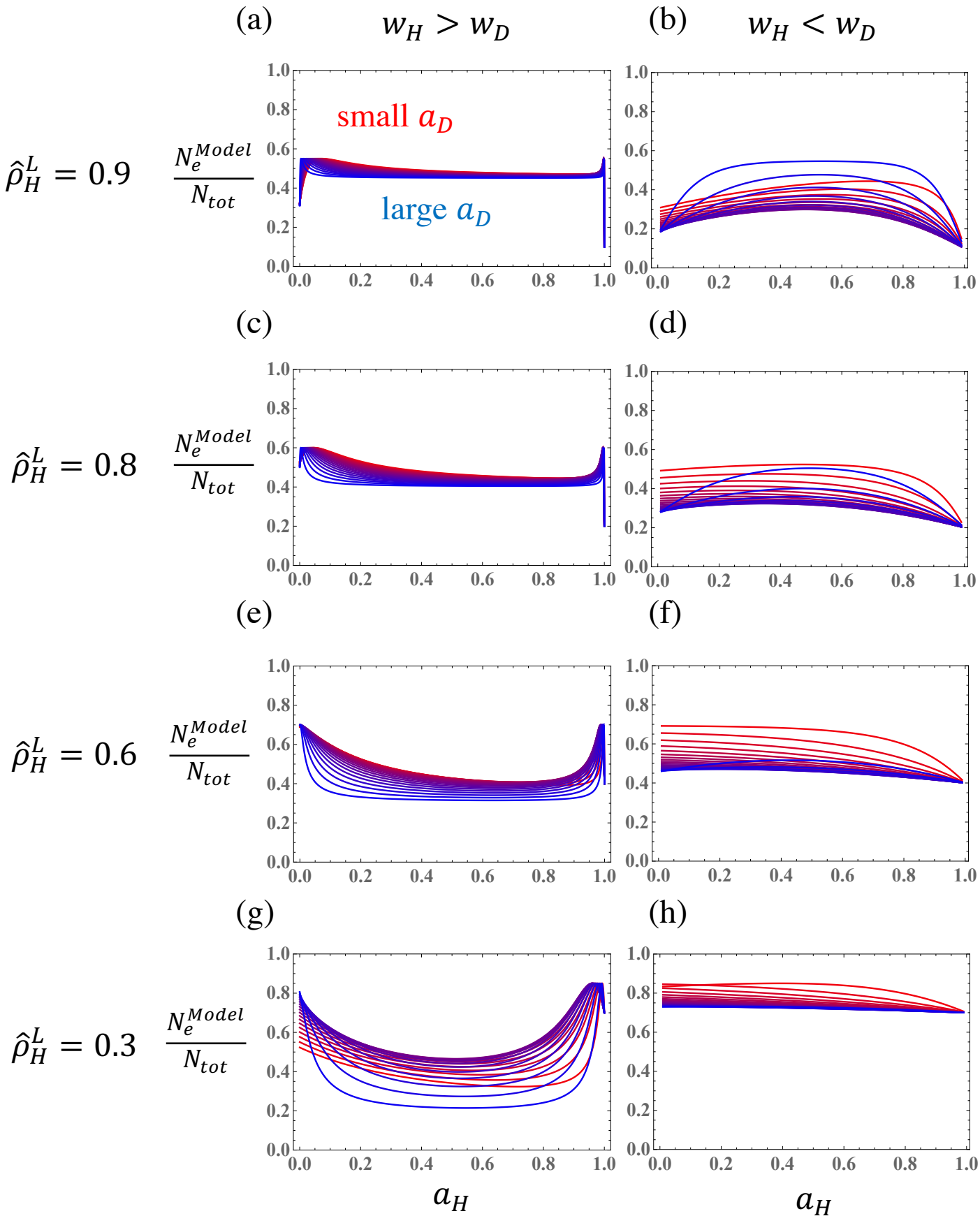
(a)
$w_H > w_D$
(b)
$w_H < w_D$
small a_D
large a_D
$\hat{\rho}_H^L = 0.9$
$\hat{\rho}_H^L = 0.8$
$\hat{\rho}_H^L = 0.6$
$\hat{\rho}_H^L = 0.3$
$\frac{N_e^{Model}}{N_{tot}}$
(c)
(d)
(e)
(f)
(g)
(h)
0.0
0.2
0.4
0.6
0.8
1.0
a_H
a_H

Figure 7

(a) global regulation

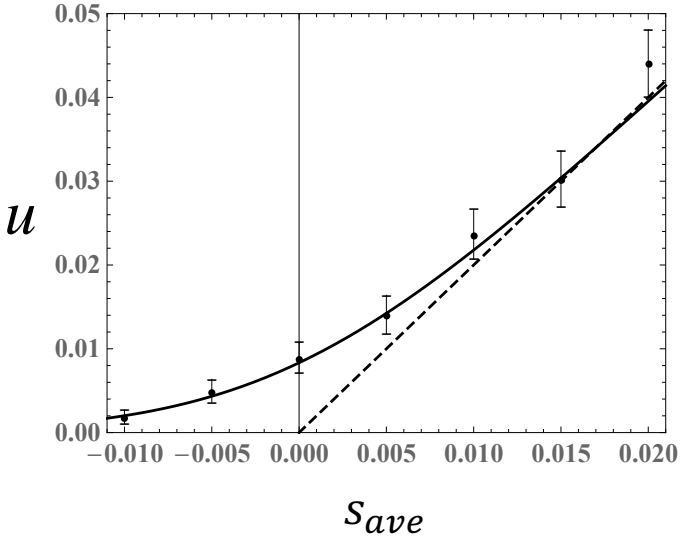

(b) local regulation

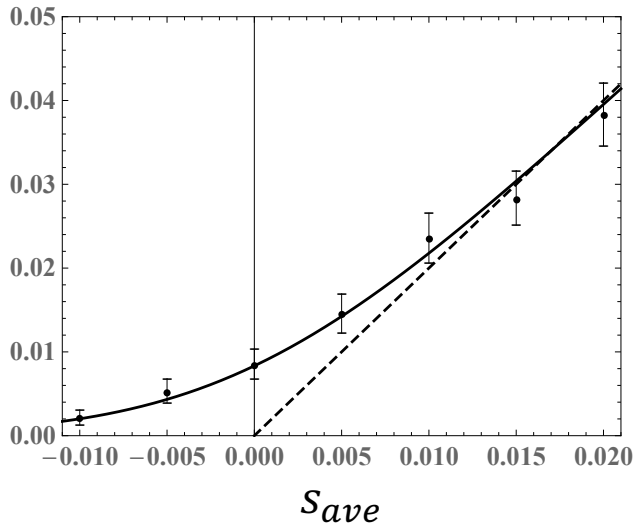

Figure 8

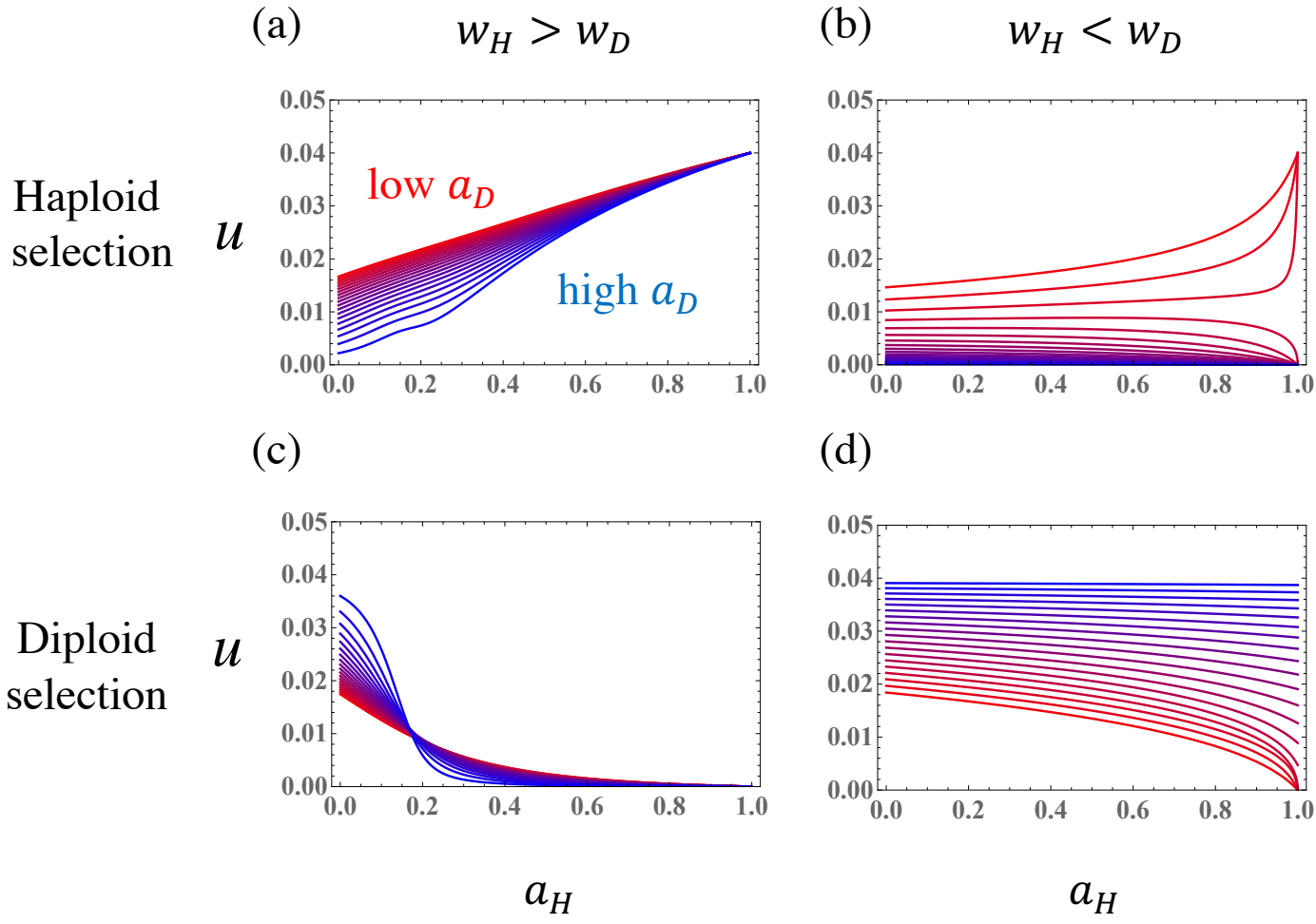

Bessho and Otto

Figure 9

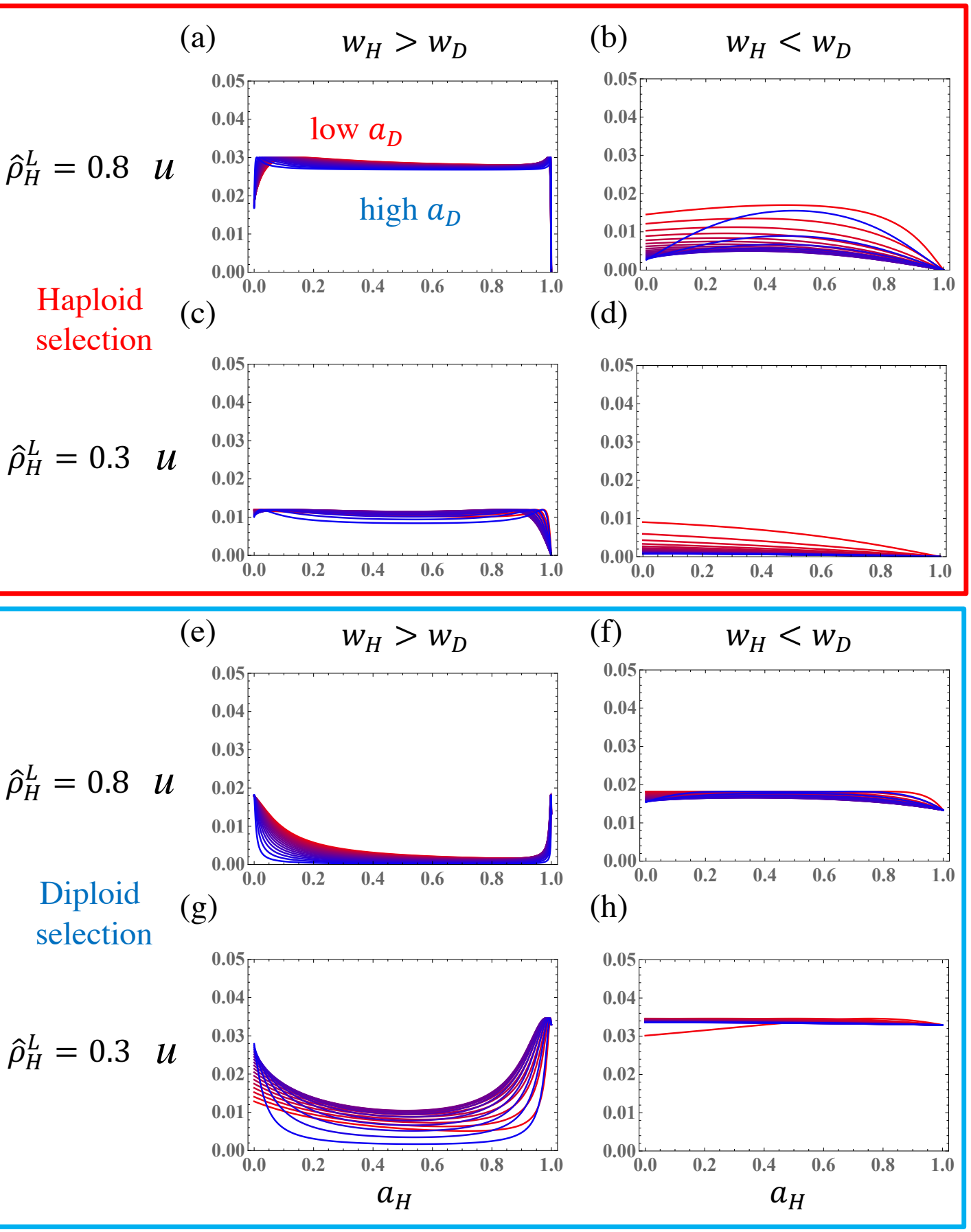
(a)
$w_H > w_D$
(b)
$w_H < w_D$
low a_D
high a_D
$\hat{\rho}_H^L = 0.8$ u
Haploid selection
(c)
(d)
$\hat{\rho}_H^L = 0.3$ u
(e)
$w_H > w_D$
(f)
$w_H < w_D$
$\hat{\rho}_H^L = 0.8$ u
Diploid selection
(g)
(h)
$\hat{\rho}_H^L = 0.3$ u
a_H
a_H